Received: 3 October 2024 | Revised: 4 March 2025 | Accepted: 4 March 2025

DOI: 10.1002/mrm.30507

RESEARCH ARTICLE

Magnetic Resonance in Medicine

Age dependency of neurometabolite T_1 relaxation times

Saipavitra Murali-Manohar[1,2] | Helge J. Zöllner[1,2] | Kathleen E. Hupfeld[1,2] | Yulu Song[1,2] | Emily E. Carter[3] | Vivek Yedavalli[1] | Steve C. N. Hui[4,5,6] | Dunja Simicic[1,2] | Aaron T. Gudmundson[1,2,7] | Gizeaddis Lamesgin Simegn[1,2] | Christopher W. Davies-Jenkins[1,2] | Georg Oeltzschner[1,2] | Eric C. Porges[3,8] | Richard A. E. Edden[1,2]

[1]Russell H. Morgan Department of Radiology and Radiological Science, Johns Hopkins University School of Medicine, Baltimore, Maryland, USA

[2]F. M. Kirby Research Center for Functional Brain Imaging, Kennedy Krieger Institute, Baltimore, Maryland, USA

[3]Department of Clinical and Health Psychology, College of Public Health and Health Professions, University of Florida, Gainesville, Florida, USA

[4]Developing Brain Institute, Children's National Hospital, Washington, DC, USA

[5]Department of Radiology, The George Washington University School of Medicine and Health Sciences, Washington, DC, USA

[6]Department of Pediatrics, The George Washington University School of Medicine and Health Sciences, Washington, DC, USA

[7]The Malone Center for Engineering in Healthcare, Johns Hopkins University, Baltimore, Maryland, USA

[8]Center for Cognitive Aging and Memory, College of Medicine, University of Florida, Gainesville, Florida, USA

Correspondence
Richard A. E. Edden, Russell H. Morgan Department of Radiology and Radiological Science, Johns Hopkins University School of Medicine, Baltimore, MD 21287-0005, USA.
Email: raee2@jhu.edu

Funding information
National Institutes of Health, Grant/Award Numbers: K00 AG068440, K99 AG080084, P41 EB031771, R00 AG062230, R01 EB016089, R01 EB023963, R21 EB033516

Abstract

Purpose: To measure T_1 relaxation times of metabolites at 3 T in a healthy aging population and investigate age dependence.

Methods: A cohort of 101 healthy adults was recruited with approximately 10 male and 10 female participants in each "decade" band: 18 to 29, 30 to 39, 40 to 49, 50 to 59, and 60+ years old. Inversion-recovery PRESS data (TE/TR: 30/2000 ms) were acquired at 8 inversion times (TIs) (300, 400, 511, 637, 780, 947, 1148, and 1400 ms) from voxels in white-matter-rich centrum semiovale (CSO) and gray-matter-rich posterior cingulate cortex (PCC). Modeling of TI-series spectra was performed in Osprey 2.5.0. Quantified metabolite amplitudes for total *N*-acetylaspartate ($tNAA_{2.0}$), total creatine at 3.0 ppm ($tCr_{3.0}$), and 3.9 ppm ($tCr_{3.9}$), total choline (tCho), myo-inositol (mI), and the sum of glutamine and glutamate (Glx) were modeled to calculate T_1 relaxation times of metabolites.

Results: T_1 relaxation times of $tNAA_{2.0}$ in CSO and $tNAA_{2.0}$, $tCr_{3.0}$, mI, and Glx in PCC decreased with age. These correlations remained significant when controlling for cortical atrophy. T_1 relaxation times were significantly different between PCC and CSO for all metabolites except $tCr_{3.0}$. We also propose linear models for predicting metabolite T_1s at 3 T to be used in future aging studies.

Conclusion: Metabolite T_1 relaxation times change significantly with age, an effect that will be important to consider for accurate quantitative MRS, particularly in studies of aging.

KEYWORDS

healthy aging, inversion recovery, magnetic resonance spectroscopy, metabolites, T_1 relaxation times

1 | INTRODUCTION

There is substantial clinical interest in understanding cellular and biochemical changes associated with brain aging.[1–7] In vivo magnetic resonance spectroscopy (MRS) offers a unique tool for non-invasively detecting signals from endogenous metabolites in the human brain. MRS is quantitative, in that metabolite levels can be determined based on the amplitude of signals in the in vivo spectrum. Although other approaches exist,[8,9] the most common (and consensus) approach to metabolite quantification is to use the endogenous water signal as an internal concentration reference.[9,10] Assuming that the concentration of MR-visible water is a known quantity in different tissue types, it is possible to infer metabolite concentrations from the relative intensity of metabolite signals with respect to the water reference signal. Successive MRS measurements are performed before the signals have fully relaxed to equilibrium to maximize signal-to-noise ratio (SNR). Data acquired before the complete recovery of the longitudinal magnetization and acquired at finite echo times (TE) are T_1- and T_2-weighted, respectively. Corrections for longitudinal (T_1) and transverse (T_2) weighting of both the metabolite and water signals are necessary to yield accurate concentration values. Therefore, the extent to which MRS can correctly quantify metabolite levels depends on knowledge of the relaxation times.

Cellular and metabolic changes that occur across the lifespan are of keen interest, both in terms of understanding healthy aging and providing a baseline from which to study disease. Previous MRS studies of the aging human brain have tended to report that levels of NAA and glutamate (Glu) decrease with age,[1,2] whereas metabolites such as Cho, Cr, and glutathione (GSH) increase[1–4] with age. One common methodological limitation for MRS studies of aging is that they either do not attempt relaxation correction or apply a single set of relaxation reference values to the whole dataset.

However, such approaches may bias study findings if this age-independent relaxation treatment is not appropriate. There is now substantial evidence that T_2 relaxation rates change with aging.[11–15] Age-related changes in T_1 relaxation have not been as extensively studied, but would similarly be expected. After inconclusive results from a 1.5 T study conducted on two different age groups,[16] there is gradually increasing evidence from another 1.5 T study[17] and our prior 3 T study[18] that T_1 relaxation times of metabolites change with age. Our recent results demonstrated significant decreases in metabolite T_1s across the adult lifespan, but were limited by a two-point methodology and only considering two metabolites.[18]

In this manuscript, a new prospective cohort (~10 females and 10 males in each decade of adult life from 20s, 30s, 40s, 50s, and 60+) was recruited to measure metabolite T_1 relaxation times across the lifespan. With the balanced age and sex makeup, this study will fill a current gap by producing age-normed reference values for quantification correction in the future. There is also a growing interest in the relaxation properties of metabolite signals,[19] not just for the purposes of quantification correction, but for information on the specific cellular environments sampled by metabolites.[20]

2 | METHODS

2.1 | Participants

A total of 101 participants were recruited for this study at two sites, the Johns Hopkins University School of Medicine (JHU) ($n = 51$) and the University of Florida (UF) ($n = 50$). The age range of the participants was balanced in such a way that it included approximately 10 females and 10 males (5 females and 5 males at each site) from age ranges: 18 to 29, 30 to 39, 40 to 49, 50 to 59, and 60+ years. All study procedures were approved by a single institutional review board (sIRB) at the JFU, with authority ceded by the UF IRB. Written informed consent was obtained from all participants. A detailed description of participant demographics can be found in Table 1. A previous publication[15] reports on metabolite T_2s from the same scan session.

2.2 | Data acquisition

MRI and MRS scans were performed using a 32-channel head coil on either a 3 T Philips dStream Ingenia Elition MRI scanner at JHU or a 3 T Philips MR7700 MRI scanner at UF. First, a T_1-weighted structural MRI (MPRAGE, TR/TE: 8.1/3.7 ms, flip angle: 8°, slice thickness: 1.0 mm, 150 slices, acquisition duration: 2 min 46 s) was acquired to facilitate voxel placement. Next, an inversion recovery series was acquired using PRESS localization (TE/TR: 30/2000 ms, chemical shift selective (CHESS) water suppression with 115 Hz bandwidth) in two voxels (size 30 (anterior-posterior AP) × 26 right-left (RL) × 26 foot-head (FH) mm^3), the white-matter-rich centrum semiovale (CSO) and the gray-matter-rich posterior cingulate cortex (PCC). The series consisted of eight logarithmically spaced TIs: 300, 400, 511, 637, 780, 947, 1148, and 1400 ms. 24 transients were acquired per TI sampled at 2000 Hz with 1024 points. A water reference TI series was acquired with the same parameters, except with only 2 transients per TI and no water suppression applied.

TABLE 1 Participant demographics.

Variable	18–29 years	30–39 years	40–49 years	50–59 years	60+ years
Sex, no.	10 F, 13 M	9 F, 10 M	10 F, 9 M	9 F, 9 M	11 F, 9 M
Age, mean (SD)	24.2 (3.3)	35.2 (2.8)	43.9 (2.9)	55.0 (2.9)	67.5 (4.1)
[Min, Max], y	[18.7, 29.8]	[31.8, 39.9]	[40.0, 48.2]	[50.2, 59.8]	[60.8, 75.4]

Abbreviations: F, female; M, male; Max, maximum; Min, minimum; SD, standard deviation.

2.3 | MRS data processing

Philips raw data were coil-combined, eddy-current-corrected and averaged within each TI on the scanner. TI-series MRS data were processed using Osprey 2.5.0, an open-source analysis toolbox for MRS data.[21] Preprocessing steps were performed on each subject, for each TI separately. All processing steps recommended in the MRS community consensus[9] were followed. The residual water signal was removed using Hankel singular value decomposition (HSVD) in Osprey. The frequency and phase drifts were corrected based on spectral registration.[22] Phase correction was performed based on the well-behaved water signal for TI 300, 400, 780, 947, 1148, and 1400 ms. The phase correction steps for TI 511 and 637 ms, which were close to the metabolite null point, were corrected manually because of low SNR for the major metabolite peaks.

2.4 | MRI segmentation

Osprey-constructed binary masks of the voxels were co-registered to the T_1-weighted structural images and segmented using SPM12[23] to yield volume fractions of white matter (fWM), gray matter (fGM), and CSF (fCSF).

2.5 | Spectral modeling

Spectral modeling was performed for each TI spectrum separately in Osprey 2.5.0 using a custom PRESS TE 30 ms basis set generated using MRSCloud[24] (https://braingps.mricloud.org/mrs-cloud) for Philips-specific sequence timings and accurate RF pulse shapes. The basis set consisted of 19 metabolite basis functions: ascorbate (Asc), aspartate (Asp), the methyl group of creatine ($CrCH_3$) at 3.0 ppm, methylene group of creatine ($CrCH_2$) at 3.9 ppm, γ-aminobutyric acid (GABA), glycerophosphocholine (GPC), GSH, glutamine (Gln), Glu, lactate (Lac), myo-inositol (mI), acetyl moiety of NAA (NAA_{ace}) at 2.01 ppm, aspartyl moiety of NAA (NAA_{asp}), acetyl moiety of *N*-acetyl aspartyl glutamate ($NAAG_{ace}$) at 2.04 ppm, aspartyl and glutamate moiety of NAAG ($NAAG_{asp\_glu}$), phosphocholine (PCh), phosphorylethanolamine (PE), scyllo-inositol (sI), taurine (Tau); 5 macromolecule basis functions: MM09, MM12, MM14, MM17, and MM20; and 3 lipid basis functions: Lip09, Lip13, and Lip20. MM and lipids were included in modeling as parameterized Gaussian basis functions.

In line with other linear combination modeling software, Osprey only allows positive coefficients for basis functions in the spectral model. This presents a challenge for modeling TI series spectra in which signals have a polarity that depends on the degree of longitudinal relaxation of the z-component during the inversion delay TI. For example, in short-TI spectra, metabolite signals appear with negative polarity, whereas macromolecule signals have already recovered past the null-point and appear with positive polarity. It is convenient for modeling to phase these spectra so that the metabolite signals are positive—therefore, macromolecule and lipid basis functions were inverted. In TI-511 spectra, macromolecule signals again appear with positive polarity, and metabolite signals are still inverted, but close to the null point. These spectra were modeled with their natural polarity, therefore, metabolite basis functions were inverted. In TI-637 spectra, the metabolite signals are very close to the null point with all but the strongest signals well below the noise level. These spectra were modeled with a reduced metabolite basis set (including only positive total Cr at 3.9 ppm ($tCr_{3.9}$), and negative total N-acetylaspartate ($tNAA_{2.0}$), total NAA_{asp} ($tNAA_{asp}$), mI, glutamine + glutamate (Glx), and total Cr at 3.0 ppm ($tCr_{3.0}$) functions) to avoid over-fitting. At long TIs, both metabolite and macromolecular signals have positive phase and modeling is straightforward. Overall, this approach can be summarized as modeling spectra phased so that the dominant component (i.e., metabolites in long- and short-TI spectra and MM in mid-TI spectra) is positive, and adjusting the polarity of basis functions of other signals as appropriate. This provided better initialization for modeling variables, which results in better optimization outcomes. Most TIs were modeled with a spline baseline knot spacing of 0.6, the default for "typical" short-TE spectra at 3 T. Mid-TI spectra (TI 511 and 637 ms) were modeled with a more flexible baseline with a knot spacing of 0.2 and without lineshape convolution beyond Gaussian and Lorentzian broadening. TI 780 ms spectra were modeled with 0.6 knot spacing and without lineshape convolution. Following spectral modeling of the metabolite TI-series,

basis function amplitude factors were extracted for T_1 modeling. Metabolite signal amplitudes for TIs 300, 400, 511, and 637 ms were multiplied by −1 as appropriate to correct for modeling of inverted spectra and/or modeling with inverted basis functions. TI-series water reference spectra were processed to have positive phase and modeled using Osprey with a simulated water basis function. Water amplitudes for T_1 modeling were extracted and polarities were corrected based on observing the phase inversion of the first point of the raw FIDs.

2.6 | T_1 relaxation modeling

For modeling T_1 relaxation times of the metabolite signals, six signals were considered: $tNAA_{2.0}$; $tCr_{3.0}$; $tCr_{3.9}$; mI; and Glx. Linear combination model metabolite amplitudes from the TI spectra for every subject were fitted in MATLAB R2022a using lsqcurvefit to the inversion recovery equation:

$$S_{\text{metabolite}} = A_{\text{metabolite}}\left(1 - 2e^{\frac{-TI}{T_1}} + e^{\frac{-TR}{T_1}}\right), \quad (1)$$

with modeled parameters T_1 and A, an amplitude factor. To calculate the T_1 relaxation time of tissue water, as distinct from CSF water, the water signal amplitudes were modeled using a two-pool inversion recovery model for the water signal S_{water}:

$$S_{\text{water}} = A_{\text{water}}\left(\left(1 - 2e^{\frac{-TI}{T_{1,tissue}}} + e^{\frac{-TR}{T_{1,tissue}}}\right)(c_{GM}f_{GM} + c_{WM}f_{WM}) + \left(1 - 2e^{\frac{-TI}{T_{1,CSF}}} + e^{\frac{-TR}{T_{1,CSF}}}\right)c_{CSF}f_{CSF}\right), \quad (2)$$

where A is an amplitude factor scaling constant, $T_{1,tissue}$ is the tissue water T_1 relaxation time, $T_{1,CSF}$ is the CSF water T_1 relaxation time and concentrations of water in respective tissue fractions are $c_{GM} = 43.3$, $c_{WM} = 36.08$ and $c_{CSF} = 53.84$ mol/kg.[10,25] A and $T_{1,tissue}$ were unconstrained whereas $T_{1,CSF}$ was constrained between 1000 and 5000 ms.

2.7 | Statistical analyses

All statistical analyses were performed in R 4.3.2[26] within RStudio[27] (and followed the identical approach used in our prior report on metabolite T_2s from the same participants[15]). The correlation between T_1 relaxation time and age for each metabolite signal was calculated for each voxel separately. Because multiple variables did not satisfy the Pearson correlation normality assumption (Shapiro test $p < 0.05$), non-parametric Spearman correlations are reported. To account for multiple comparisons, Benjamini-Hochberg false discovery rate (FDR) correction was applied to the p-values. A linear model was calculated for each signal with T_1 as the outcome variable and age-minus-30 as the predictor: $T_1 = \beta_o + \beta_1 \times (\text{Age} - 30)$. The intercept from this model represents the predicted T_1 at 30 years of age, and the slope represents the change in T_1 for each year of age. For significant correlations between T_1 and age, additional analyses were performed controlling the linear models for cortical atrophy: $T_1 = \beta_o + \beta_1 \times (\text{Age} - 30) + \beta_2 \times \text{Tissue}$, using the gray matter tissue fraction (i.e., $\text{Tissue} = f_{GM}/(f_{GM} + f_{WM})$) to represent the expected loss of cortical GM with age. Two-sample t tests were used to assess possible sex differences in T_1 relaxation times in each voxel. Finally, to test for differences in T_1 relaxation times between the voxels, paired t tests were performed, followed by correction for multiple comparisons.

3 | RESULTS

3.1 | Data quality

CSO and PCC voxel locations are shown in Figure 1. Voxel tissue fractions were: for CSO, fGM 0.24 ± 0.07,

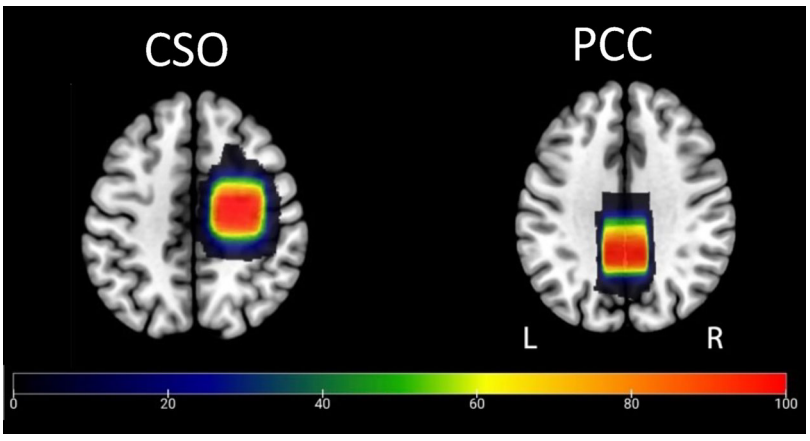

FIGURE 1 Voxel placement for TI series data acquisition. Voxels of size $30 \times 26 \times 26$ mm^3 were placed in the CSO and PCC regions. This figure illustrates the areas of overlap in the voxel placements across subjects. The native space binary voxel mask from each participant was normalized to standard Montreal Neurological Institute (MNI) space and overlaid onto the spm152 template. The color bar indicates the number of subjects overlapped, from 0 (blue) to all subjects (red).

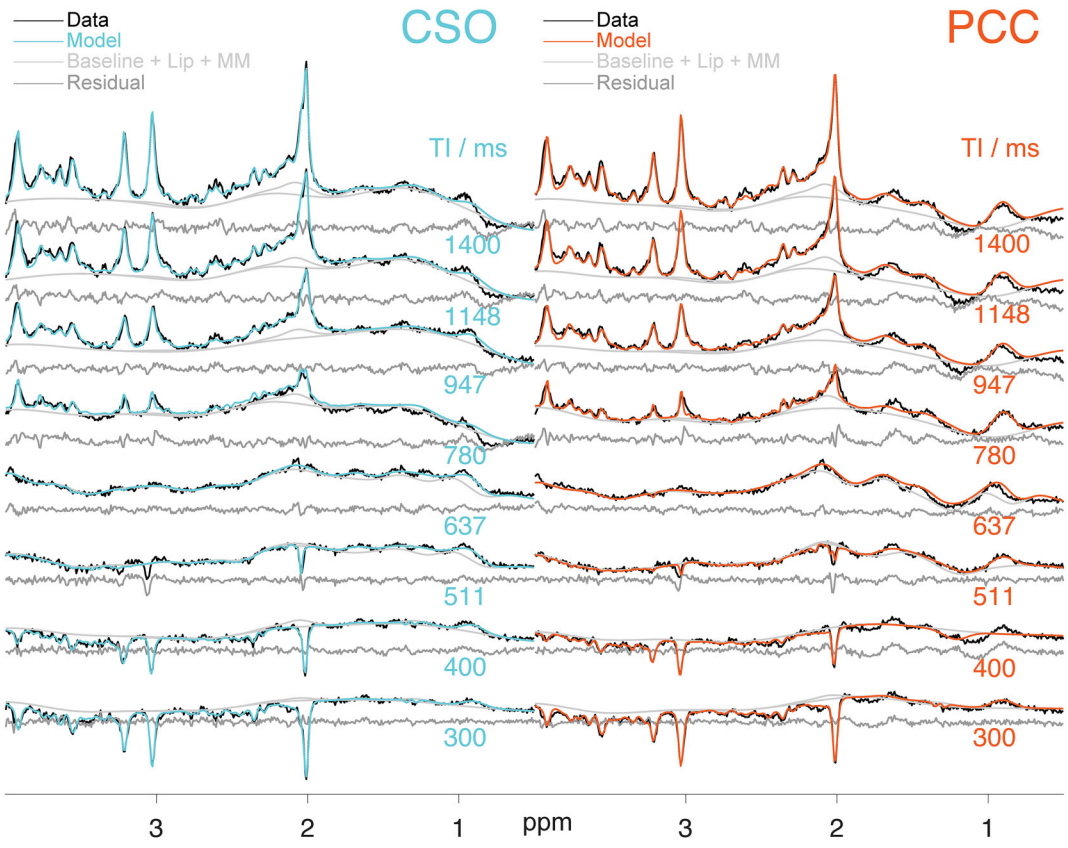

FIGURE 2 Inversion recovery PRESS spectra, models and fit residuals from a representative subject (58-year-old-female) for all 8 TIs from the CSO and the PCC regions. This subject was determined from the median value of average R^2 of T_1 curve model fit for all 6 metabolites and tissue water.

fWM 0.70 ± 0.10, and fCSF 0.06 ± 0.04, and for PCC, fGM 0.58 ± 0.06, fWM 0.25 ± 0.06, and fCSF 0.17 ± 0.07. Four datasets were excluded: one because of large frequency drifts across transients and lipid artifacts (49-year-old male), one because of an acquisition error with wrong inversion offset (30-year-old female), and one because of poor linewidth (66-year-old male). For one 19-year-old male, the PCC voxel was placed in the wrong location and that dataset was also excluded. Representative median inversion recovery series spectra from CSO and PCC are shown in Figure 2. $tCr_{3.0}$ linewidths for CSO and PCC were 9 ± 2 and 7 ± 2 Hz for TI 1400 ms spectra. SNR of $tCr_{3.0}$ peak for TI 1400 ms spectra measured from CSO and PCC were 62 ± 10 and 67 ± 14, respectively. The goodness of fit for the spectral modeling was evaluated by the ratio of the peak residual to the standard deviation of the noise. When ≫1, then it indicates unmodeled peaks in the fit that can include lipid peaks and/or macromolecular contributions. The ratios were 2.12 ± 1.29, 1.94 ± 1.17, 3.05 ± 1.56, 8.18 ± 15.43, 10.24 ± 10.83, 9.28 ± 13.15, 9.48 ± 10.78, and 11.24 ± 11.35 for TIs 300, 400, 511, 637, 780, 947, 1148, and 1400 ms, respectively, in CSO; 2.39 ± 0.82, 4.27 ± 3.79, 7.06 ± 32.06, 6.47 ± 8.84, 8.40 ± 6.10, 7.45 ± 8.99, 8.78 ± 12.19, and 13.02 ± 22.16 in PCC. Higher ratio for TIs closer to the metabolite-null point arises because of the fact that the convolution term was removed in the modeling of these TIs. Hence, it resulted in missing or incompletely modeling some signal. T_1 relaxation curves for the six metabolite signals and tissue water are shown in Figure 3 for both CSO and PCC voxels from the same subject. Mean R^2 values for all the metabolites and water across all the subjects were 0.94 or greater than as a measure of goodness of fit for the T_1 exponential curves. Table 2 provides mean values and standard deviations (grouped by age) of T_1 relaxation times for the seven signals from CSO and PCC.

3.2 | T_1 correlations with age

Correlation plots between T_1 relaxation times and age are presented in Figure 4. Spearman correlation coefficients and FDR-corrected *p*-values are given in Table 3. T_1 relaxation times decreased significantly with age for $tNAA_{2.0}$, $tCr_{3.0}$, mI, and Glx in PCC, whereas only for $tNAA_{2.0}$ in CSO. Among the significant correlations ($p < 0.05$, FDR

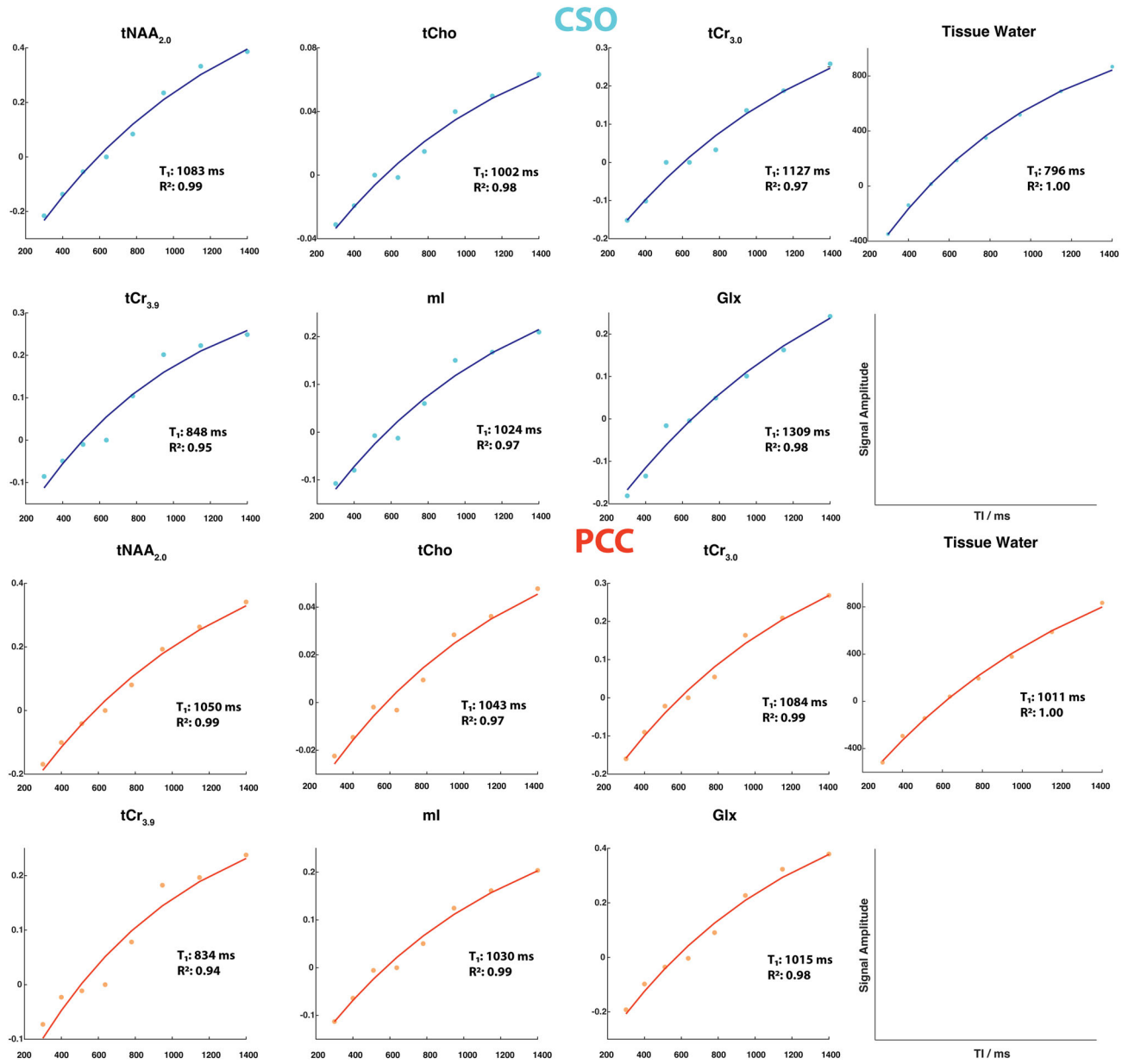

FIGURE 3 T_1 relaxation curves for 6 metabolite signals and tissue water from the same subject represented in Figure 2. Points represent the metabolite amplitudes modeled at each TI and solid lines represent the T_1 relaxation model of best fit as calculated using the inversion recovery signal equation given in Eq. (1). T_1 relaxation times for each metabolite for this subject are provided in the plot along with the R^2 values as a measure of goodness of fit for the curves.

corrected), Spearman coefficients ranged from −0.23 for mI in PCC to −0.69 for NAA in PCC. Tissue water T_1 did not correlate significantly with age in CSO or PCC. When controlling for cortical atrophy, correlations of T_1 with age remained significant for each of the four metabolite signals in PCC and for $tNAA_{2.0}$ in CSO. No sex differences in T_1 relaxation times of metabolites or tissue water were observed for either region.

T_1 can be predicted for each metabolite from the linear model $T_1 = \beta_o + \beta_1 \times (\text{Age} - 30)$. Table 4 gives the T_1-intercept at 30 years of age (β_o), and the slope (β_1), which represents the change in predicted T_1 for each year of life. Slopes are only reported for the cases where T_1 was significantly correlated with age. These linear models are represented as the gray trend lines in Figure 4.

3.3 | T_1 Differences by Voxel

Box plots comparing T_1 relaxation times for the CSO and PCC voxels are shown in Figure 5. They were significantly different between the voxels for all metabolites, except

TABLE 2 Mean T_1 relaxation times in milliseconds for metabolites and tissue water grouped by age.

Metabolite	18–29 years	30–39 years	40–49 years	50–59 years	60+ years
CSO Voxel					
$tNAA_{2.0}$	1173	1143	1150	1130	1094
	(41)	(45)	(45)	(48)	(42)
$tCr_{3.0}$	1123	1119	1118	1110	1086
	(58)	(66)	(65)	(40)	(58)
$tCr_{3.9}$	878	861	876	864	857
	(34)	(39)	(36)	(29)	(35)
tCho	1034	1026	1028	1031	1012
	(28)	(34)	(33)	(27)	(41)
mI	1022	1039	1017	1035	995
	(31)	(53)	(33)	(24)	(36)
Glx	1327	1382	1287	1297	1423
	(145)	(222)	(95)	(161)	(382)
Tissue water	771	726	746	777	807
	(104)	(97)	(45)	(54)	(111)
PCC Voxel					
$tNAA_{2.0}$	1144	1112	1106	1071	1052
	(45)	(36)	(35)	(30)	(38)
$tCr_{3.0}$	1112	1113	1095	1095	1086
	(35)	(53)	(46)	(19)	(37)
$tCr_{3.9}$	821	825	838	832	835
	(30)	(36)	(39)	(22)	(35)
tCho	1041	1045	1043	1036	1036
	(43)	(44)	(48)	(22)	(35)
mI	1068	1068	1054	1039	1052
	(48)	(53)	(26)	(20)	(41)
Glx	1173	1206	1120	1098	1102
	(77)	(107)	(122)	(75)	(84)
Tissue water	959	944	942	935	949
	(124)	(144)	(87)	(76)	(65)

Note: Standard deviations are provided in parentheses.

Abbreviations: CSO, centrum semiovale; Glx, the sum of glutamine and glutamate; mI, myo-inositol; PCC, posterior cingulate cortex; tCho, total choline; $tCr_{3.0}$, total creatine at 3.0 ppm; $tCr_{3.9}$, total creatine at 3.9 ppm; $tNAA_{2.0}$, N-acetylaspartate.

$tCr_{3.0}$. T_1 values were higher for $tNAA_{2.0}$, $tCr_{3.9}$, and Glx in CSO, but higher for tCho, mI, and tissue water in PCC.

4 | DISCUSSION

This study investigated changes in T_1 relaxation times of metabolites and tissue water across the adult lifespan, with participants between 18 and 75 years of age. This cohort of 101 subjects is by far the largest dataset to analyze metabolite T_1 changes with age. Data were acquired in two regions, white matter (WM)-rich CSO and gray matter (GM)-rich PCC, which enabled an examination of the differences between WM and GM tissues. The T_1 relaxation times of most metabolites decreased significantly with age in PCC. However, in CSO, only $tNAA_{2.0}$ decreased significantly with age. T_1 relaxation times of tissue water did not change significantly in CSO or PCC, although showed a strong positive trend with age in CSO and a weak positive trend in PCC.

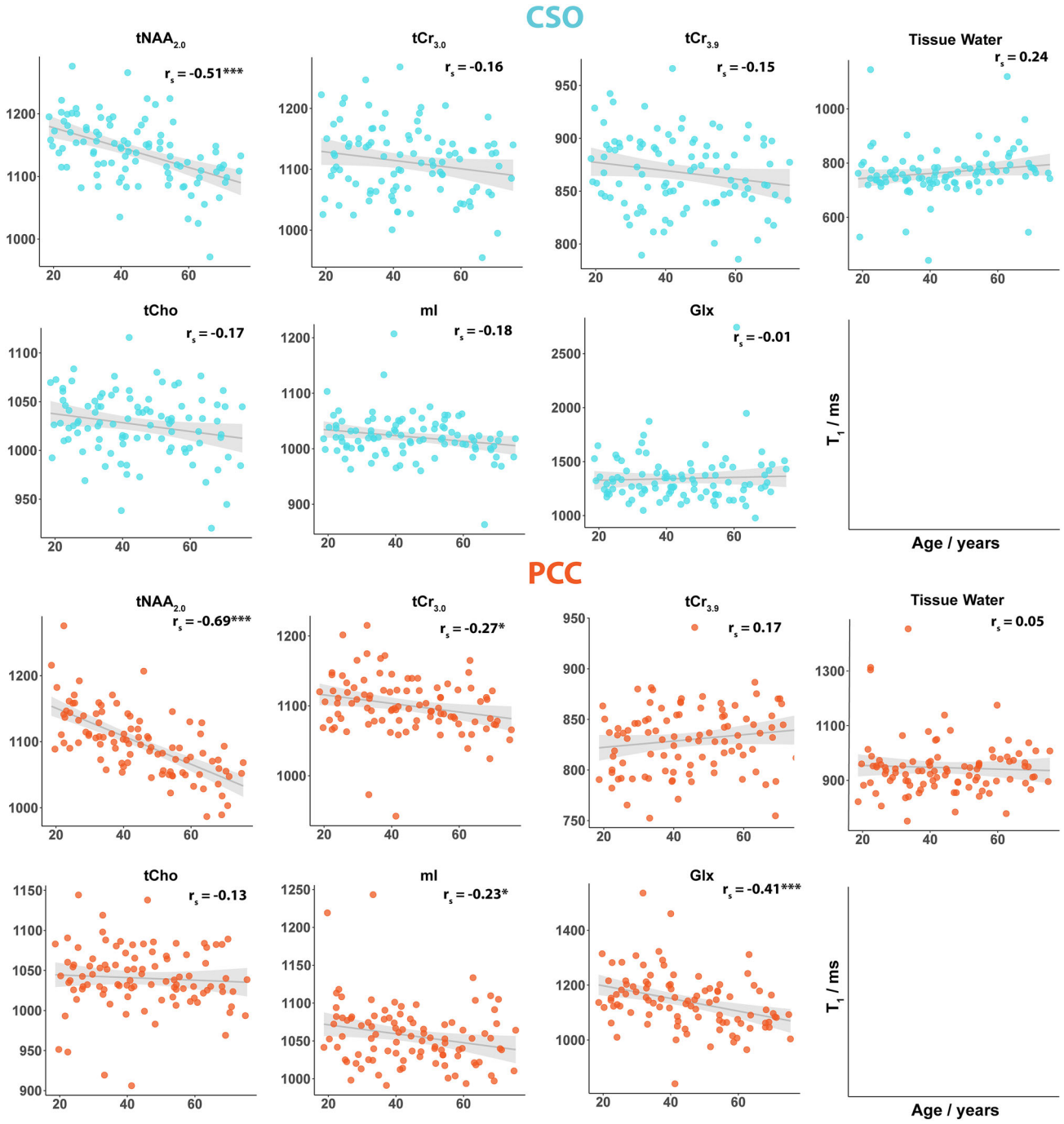

FIGURE 4 Age-T_1 correlation plots are shown for all six metabolites and tissue water from both centrum semiovale (CSO) (blue) and posterior cingulate cortex (PCC) (orange). Spearman correlation coefficient for each plot is indicated in the top-right corner with false discovery rate-corrected *p*-value for the correlation $*p < 0.05$, $**p < 0.01$, $***p < 0.001$. The gray line and shading represent the linear model and 95% confidence interval for the model using age to predict T_1 (produced using the *geom_smooth* function in R).

To date, few studies[16–18] have investigated the impact of aging on metabolite T_1 relaxation. Early research performed at 1.5 T was inconsistent with one study showing no changes[16] and one showing decreases with age[17] for $tNAA_{2.0}$ and $tCr_{3.0}$ in CSO. In the current 3 T study, T_1 relaxation times decreased significantly with age in PCC for the singlets, $tNAA_{2.0}$, and $tCr_{3.0}$, as well as the multiplets, mI, and Glx. In the CSO, significant decreases were only observed for $tNAA_{2.0}$. These results, using a more sophisticated measurement protocol, reproduce and build on our previous findings[18] of decreasing metabolite T_1 with age for $tNAA_{2.0}$ and $tCr_{3.0}$. The age-related change in T_1 relaxation times, when comparing 25-years-old to 65-years-old from the linear models

TABLE 3 Spearman correlation coefficients (r_s) of T_1 with age and FDR-corrected p-values.

	CSO		PCC	
Metabolite	r_s	$p_{FDR\text{-}corr}$	r_s	$p_{FDR\text{-}corr}$
$tNAA_{2.0}$	−0.51	6.48×10^{-7}***	−0.69	6.40×10^{-14}***
$tCr_{3.0}$	−0.16	0.16	−0.27	0.017*
$tCr_{3.9}$	−0.15	0.16	0.17	0.15
tCho	−0.17	0.16	−0.13	0.25
mI	−0.18	0.16	−0.23	0.04*
Glx	−0.01	0.91	−0.41	1.26×10^{-4}***
Tissue water	0.24	0.06	0.05	0.70

Abbreviations: CSO, centrum semiovale; FDR-corr, false discovery rate corrected; Glx, the sum of glutamine and glutamate; mI, myo-inositol; PCC, posterior cingulate cortex; tCho, total choline; $tCr_{3.0}$, total creatine at 3.0 ppm; $tCr_{3.9}$, total creatine at 3.9 ppm; $tNAA_{2.0}$, N-acetylaspartate.
*$p < 0.05$. **$p < 0.01$. ***$p < 0.001$ for CSO and PCC.

TABLE 4 Linear model coefficients, namely intercept (in ms) and slope (in ms/year), for estimating T_1 relaxation times for a given age using $T_1 = \beta_o + \beta_1 \times (\text{Age} - 30)$.

	CSO		PCC	
Metabolite	**Intercept**	**Slope (β_1)**	**Intercept**	**Slope (β_1)**
$tNAA_{2.0}$	1162	−1.58	1130	−2.12
$tCr_{3.0}$	1122		1110	−0.61
$tCr_{3.9}$	873		825	
tCho	1033		1043	
mI	1029		1065	−0.59
Glx	1334		1175	−2.31
Tissue water	753		951	

Note: Slope is provided only for those metabolites where T_1 was significantly correlated with age; slope represents change in predicted T_1 with each year of life beyond 30 years of age. Intercept values correspond to predicted T_1 values for age = 30 years.
Abbreviations: CSO, centrum semiovale; Glx, the sum of glutamine and glutamate; mI, myo-inositol; PCC, posterior cingulate cortex; tCho, total choline; $tCr_{3.0}$, total creatine at 3.0 ppm; $tC_{r3.9}$, total creatine at 3.9 ppm; $tNAA_{2.0}$, *N*-acetylaspartate.

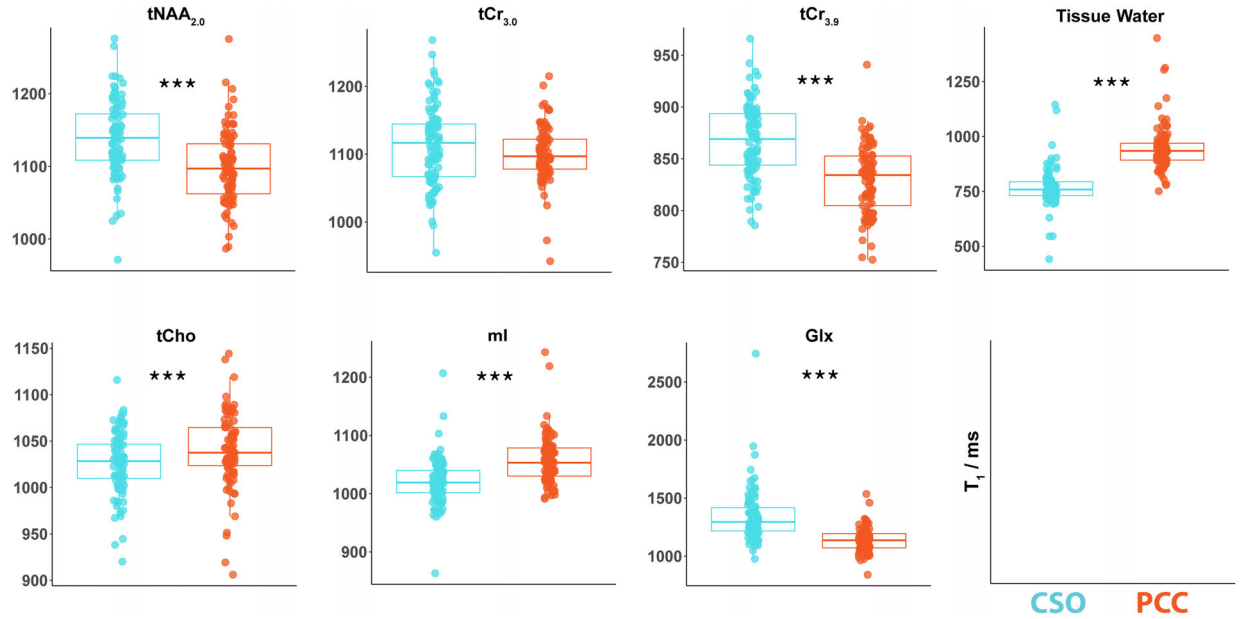

FIGURE 5 Differences in T_1 relaxation times between CSO (blue) and PCC (orange). Each datapoint for CSO and PCC represents one participant. The asterisks indicate the statistical significance of the false discovery rate-corrected p-value for the paired t-test, *$p < 0.05$, **$p < 0.01$, ***$p < 0.001$.

(Figure 4, Table 4), range from 2% to 8%. Considering the impact of these differences for a typical acquisition TR of 2 s, these values correspond to a change in T_1 correction factor $1/(1-\exp(-TR/T_1))$ range of between 0.8% to 3.0%. These effects are smaller at TR 3.0 s and larger at TR 1.5 s, to mention two other commonly used TRs. Although these effects are modest, they are sufficiently large to merit consideration, particularly in the context of MRS studies of aging that are often under-powered, and these effects may result in marginal impacts on statistical significance, especially when combined with other relevant factors, including age related changes in metabolite T_2, and in water relaxation and MR-visible concentration.

There is a more substantial quantitative imaging literature on trends in water T_1 relaxation times with age. One such study showed significant increases in T_1 relaxation times of tissue water across various subcortical, cortical, and cerebellar brain regions[28] in a cohort between 18 and 78 years old. Another study of 211 subjects between 20 and 89 years showed positive correlations between age and water T_1 in the frontal WM, globus pallidus, and genu of the corpus callosum, whereas showed negative linear correlations subcortically in the thalamus, head of the caudate nucleus, and putamen.[29] Water T_1s in the brain are generally thought to be influenced by myelination, iron deposition, and water content. These three factors have been shown to vary with age—myelin and water content decrease with age,[29,30] whereas iron accumulates with age.[28,29] Demyelination prolongs T_1 relaxation times,[31,32] whereas reduction in water content and increase in iron content reduces T_1 relaxation times.[33,34] In the current study, the T_1 of tissue water increases (but not to a significant degree), and more strongly in CSO, possibly reflecting the demyelination associated with aging.[35,36] The difference between PCC and CSO could also reflect the greater influence of iron in GM regions.[29] Metabolites are predominantly intracellular, absent from CSF and present at different levels in different cell types. Although the localization of metabolites and water differs, the underlying mechanisms of T_1 relaxation will be similar, but may be weighted differently. The general trend of metabolite T_1s to decrease with age (whereas water T_1s tends in general to increase) suggests that the reduction in water content intracellularly and the increase in iron content may have a relatively greater impact on metabolite signals than water.

Several studies have previously measured T_1 relaxation times of metabolites in both GM and WM regions at various field strengths. Overall, the differences between GM and WM T_1 for metabolites reported here are consistent with literature. In our study, $tNAA_{2.0}$ had a longer T_1 in WM than in GM, with similar trends reviously described.[37–40] However, some studies[41,42] reported slightly higher NAA T_1s in GM than in WM. No significant difference was found in $tCr_{3.0}$ values between WM and GM in our study, and this was in line with most previous findings.[37–40,43] Where tissue differences in tCho T_1s are reported, they tend to be higher in GM,[38,39,41] which is in agreement with our results. Glx has higher T_1 in WM than in GM in the current study similar to previous reports.[38,40] The T_1 relaxation time of mI is higher in GM in our study.[39,40] Some inconsistencies are seen in the trends reported here compared to previous literature. These differences can be attributed to differences in measurement method used viz., inversion recovery or saturation recovery, and differences in the spectral modeling routine used. Tissue water T_1 is generally shorter in WM, as indicated in the current study, and in agreement at 3 T[39] and 7 T[38] as well as in several non-MRS methods.[44–46] As discussed above, this is likely driven by the higher myelin content in the CSO,[47–49] accelerating relaxation processes and resulting in shorter T_1 times.[50,51] It is particularly interesting that one set of metabolites (tNAA, tCr, and Glx) show higher T_1s in CSO and another (tCho and mI) lower. In terms of their roles and cell type, tNAA and Glx are more closely associated with neuronal energy and neurotransmission metabolism, whereas tCho and mI are more associated with the glial compartment.[52] Overall, the variability in metabolite T_1 relaxation times between WM-rich CSO and GM-rich PCC across these studies reflects the inherent differences in brain tissue composition, the influence of magnetic field strength, and measurement techniques.

This study has a number of limitations. First, modeling of the TI series data was challenging, especially in TIs that are close to metabolite null-points because these spectra had larger MM signals than metabolite signals. The lack of prior knowledge in MM makes it difficult to clean the spectra. Given that our focus here was metabolite T_1s, we relied on a spline baseline to model much of the MM contribution to the spectrum, especially at TI 511 and 637 ms, where a more flexible spline baseline was used. Methodologically, it is not ideal to use different model settings for different spectra within a dataset, but given the drastically different character of these mid-TI spectra, it was necessary to give plausible spectral models and metabolite amplitudes that were coherent with the inversion-recovery curve established by the long- and short-TI extremes. Turning off the convolution was also necessary for model convergence, but makes it harder to "find" peaks and model them. As a result, some peaks are missed. It is a limitation of the amplitude estimation, but a very small positive, zero, or very small negative signal for mid-TIs does not tend to swing the T_1 model by much. Reliance on spline and parametrized MM signals has the potential for overfitting, compared to for example

using acquired MM background spectra, but no multi-TI reference dataset for MM spectra is available.[40] Second, stemming from the limited resolution of MRS, is whether the changes in CSO and PCC reflect general changes in WM and GM tissue respectively, or whether they arise from tissue sampling drift with age. We have attempted to address this limitation using a statistical covariate, but this relies on the segmentation of T_1-weighted structural MRI, which might itself be biased as water T_1s change with age and image contrast diminishes. Thirdly, the coverage of this study is limited to just two regions (which may or may not be more broadly representative of cortical GM and WM regions); future work should extend this study to other brain regions. One final limitation is the difficulty of modeling the inversion series spectra reliably, which is reflected in the varied conclusions in prior literature[16–18] discussed above. It is likely that 2D modeling[53–56] of the spectra is a more parsimonious and SNR-efficient approach for such datasets. Knowledge can then be shared across TI points, for example, the lineshapes strongly established in long-TI spectra will be constrained for low-SNR mid-TI spectra. However, implementation of a 2D modeling framework is itself not trivial and raises a number of additional decisions about how and whether to share parameters across TIs.

5 | CONCLUSION

We report decreasing metabolite T_1 with age from a large-cohort MRS measurement. This was seen more consistently in the GM-rich PCC than the WM-rich CSO. These results reflect under-studied changes in the cellular microenvironment in the human brain with healthy aging attributed to factors such as myelination, iron deposition and reduced water content. We also provide linear models to predict age-dependent metabolite T_1s for quantification relaxation correction in future MRS studies.

ACKNOWLEDGMENTS

We acknowledge Peter B. Barker for thoughtful discussions. This work was supported by National Institutes of Health grants R01 EB016089, R01 EB023963, R00 AG062230, R21 EB033516, K99 AG080084, K00AG068440, and P41 EB031771.

CONFLICT OF INTEREST STATEMENT

The authors have no conflict of interest.

ORCID

Saipavitra Murali-Manohar https://orcid.org/0000-0002-4978-0736
Helge J. Zöllner https://orcid.org/0000-0002-7148-292X
Steve C. N. Hui https://orcid.org/0000-0002-1523-4040
Dunja Simicic https://orcid.org/0000-0002-6600-2696
Aaron T. Gudmundson https://orcid.org/0000-0001-5104-0959
Georg Oeltzschner https://orcid.org/0000-0003-3083-9811
Richard A. E. Edden https://orcid.org/0000-0002-0671-7374

REFERENCES

1. Cleeland C, Pipingas A, Scholey A, White D. Neurochemical changes in the aging brain: a systematic review. *Neurosci Biobehav Rev*. 2019;98:306-319. doi:10.1016/j.neubiorev.2019.01.003
2. Haga KK, Khor YP, Farrall A, Wardlaw JM. A systematic review of brain metabolite changes, measured with 1H magnetic resonance spectroscopy, in healthy aging. *Neurobiol Aging*. 2009;30:353-363. doi:10.1016/j.neurobiolaging.2007.07.005
3. Gong T, Hui SCN, Zöllner HJ, et al. Neurometabolic time-course of healthy aging. *Neuroimage*. 2022;264:119740. doi:10.1016/j.neuroimage.2022.119740
4. Hupfeld KE, Hyatt HW, Alvarez Jerez P, et al. In vivo brain glutathione is higher in older age and correlates with mobility. *Cereb Cortex*. 2021;31:4576-4594. doi:10.1093/cercor/bhab107
5. Chang L, Ernst T, Poland RE, Jenden DJ. *In vivo* proton magnetic resonance spectroscopy of the normal aging human brain. *Life Sci*. 1996;58:2049-2056. doi:10.1016/0024-3205(96)00197-X
6. Angelie E, Bonmartin A, Boudraa A, Gonnaud PM, Mallet JJ, Sappey-Marinier D. Regional differences and metabolic changes in Normal aging of the human brain: proton MR spectroscopic imaging study. *Am J Neuroradiol*. 2001;22:119-127.
7. Grachev ID, Swarnkar A, Szeverenyi NM, Ramachandran TS, Apkarian AV. Aging alters the multichemical networking profile of the human brain: an in vivo1H-MRS study of young versus middle-aged subjects. *J Neurochem*. 2001;77:292-303. doi:10.1046/j.1471-4159.2001.00238.x
8. Heinzer-Schweizer S, De Zanche N, Pavan M, et al. In-vivo assessment of tissue metabolite levels using 1H MRS and the electric REference to access in vivo concentrations (ERETIC) method. *NMR Biomed*. 2010;23:406-413. doi:10.1002/nbm.1476
9. Near J, Harris AD, Juchem C, et al. Preprocessing, analysis and quantification in single-voxel magnetic resonance spectroscopy: experts' consensus recommendations. *NMR Biomed*. 2021;34:e4257. doi:10.1002/nbm.4257
10. Gasparovic C, Song T, Devier D, et al. Use of tissue water as a concentration reference for proton spectroscopic imaging. *Magn Reson Med*. 2006;55:1219-1226. doi:10.1002/mrm.20901
11. Deelchand DK, McCarten JR, Hemmy LS, Auerbach EJ, Eberly LE, Marjańska M. Changes in the intracellular microenvironment in the aging human brain. *Neurobiol Aging*. 2020;95:168-175. doi:10.1016/j.neurobiolaging.2020.07.017
12. Jiru F, Skoch A, Wagnerova D, et al. The age dependence of T $_2$ relaxation times of N-acetyl aspartate, creatine and choline in the human brain at 3 and 4T. *NMR Biomed*. 2016;29:284-292. doi:10.1002/nbm.3456
13. Kirov II, Fleysher L, Fleysher R, Patil V, Liu S, Gonen O. Age dependence of regional proton metabolites T 2 relaxation times in the human brain at 3 T. *Magn Reson Med*. 2008;60:790-795. doi:10.1002/mrm.21715

14. Marjańska M, Emir UE, Deelchand DK, Terpstra M. Faster metabolite 1H transverse relaxation in the elder human brain. *PLoS One*. 2013;8:e77572.
15. Hupfeld KE, Murali-Manohar S, Zöllner HJ, et al. Metabolite T2 Relaxation Times Decrease across the Adult Lifespan in a Large Multi-Site Cohort. Magn Reson Med. 2025;93(3): 916–929. doi:10.1101/2024.06.19.599719
16. Christiansen P, Toft P, Larsson HBW, Stubgaard M, Henriksen O. The concentration of *N*-acetyl aspartate, creatine + phosphocreatine, and choline in different parts of the brain in adulthood and senium. *Magn Reson Imaging*. 1993;11:799-806. doi:10.1016/0730-725X(93)90197-L
17. Kreis R, Slotboom J, Hofmann L, Chris Boesch C. Integrated data acquisition and processing to determine metabolite contents, relaxation times, and macromolecule baseline in single examinations of individual subjects. *Magn Reson Med.* 2005;54:761-768. https://onlinelibrary.wiley.com/doi/full/10.1002/mrm.20673.
18. Murali-Manohar S, Gudmundson AT, Hupfeld KE, et al. Metabolite T1 relaxation times decrease across the adult lifespan. *NMR Biomed*. 2024;37:e5152. doi:10.1002/nbm.5152
19. Kulpanovich A, Tal A. What is the optimal schedule for multiparametric MRS? A magnetic resonance fingerprinting perspective. *NMR Biomed*. 2021;34:e4196. doi:10.1002/nbm.4196
20. Ronen I, Valette J. Diffusion-weighted magnetic resonance spectroscopy. *eMagRes*. John Wiley & Sons, Ltd; 2015:733-750. doi:10.1002/9780470034590.emrstm1471
21. Oeltzschner G, Zöllner HJ, Hui SCN, et al. Osprey: open-source processing, reconstruction & estimation of magnetic resonance spectroscopy data. *J Neurosci Methods*. 2020;343:108827. doi:10.1016/j.jneumeth.2020.108827
22. Mikkelsen M, Tapper S, Near J, Mostofsky SH, Puts NAJ, Edden RAE. Correcting frequency and phase offsets in MRS data using robust spectral registration. *NMR Biomed*. 2020;33:e4368. doi:10.1002/nbm.4368
23. Ashburner J, Barnes G, Chen CC, et al. SPM12 Manual. October 15, 2021.
24. Hui SCN, Saleh MG, Zöllner HJ, et al. MRSCloud: a cloud-based MRS tool for basis set simulation. *Magn Reson Med*. 2022;88:1994-2004. doi:10.1002/mrm.29370
25. Ernst T, Kreis R, Ross BD. Absolute quantitation of water and metabolites in the human brain. I. Compartments and water. *J Magn Reson B*. 1993;102:1-8. doi:10.1006/jmrb.1993.1055
26. R Core Team. *A Language and Environment for Statistical Computing*; R Foundation for Statistical Computing; 2021 Accessed September 16, 2024. https://cir.nii.ac.jp/crid/1370298757441457025
27. RStudio Team. *RStudio: Integrated Development Environment for R*; RStudio, PBC; 2021 Accessed September 16, 2024. https://cir.nii.ac.jp/crid/1370580232391041538
28. AKTAŞ DİNÇER H, AĞILDERE AM, GÖKÇAY D. T1 relaxation time is prolonged in healthy aging: a whole brain study. *Turk J Med Sci*. 2023;53:675-684. doi:10.55730/1300-0144.5630
29. Kupeli A, Kocak M, Goktepeli M, Karavas E, Danisan G. Role of T1 mapping to evaluate brain aging in a healthy population. *Clin Imaging*. 2020;59:56-60. doi:10.1016/j.clinimag.2019.09.005
30. Lutti A, Dick F, Sereno MI, Weiskopf N. Using high-resolution quantitative mapping of R1 as an index of cortical myelination. *Neuroimage*. 2014;93:176-188. doi:10.1016/j.neuroimage.2013.06.005
31. Stüber C, Morawski M, Schäfer A, et al. Myelin and iron concentration in the human brain: a quantitative study of MRI contrast. *Neuroimage*. 2014;93:95-106. doi:10.1016/j.neuroimage.2014.02.026
32. Geyer S, Weiss M, Reimann K, Lohmann G, Turner R. Microstructural Parcellation of the human cerebral cortex – from Brodmann's post-mortem map to in vivo mapping with high-field magnetic resonance imaging. *Front Hum Neurosci*. 2011;5:1–7. doi:10.3389/fnhum.2011.00019
33. Neeb H, Zilles K, Shah NJ. Fully-automated detection of cerebral water content changes: study of age- and gender-related H_2O patterns with quantitative MRI. *Neuroimage*. 2006;29:910-922. doi:10.1016/j.neuroimage.2005.08.062
34. Ogg RJ, Steen RG. Age-related changes in brain T1 are correlated with iron concentration. *Magn Reson Med*. 1998;40:749-753. doi:10.1002/mrm.1910400516
35. Branzoli F, Ercan E, Valabrègue R, et al. Differentiating between axonal damage and demyelination in healthy aging by combining diffusion-tensor imaging and diffusion-weighted spectroscopy in the human corpus callosum at 7 T. *Neurobiol Aging*. 2016;47:210-217. doi:10.1016/j.neurobiolaging.2016.07.022
36. Bennett IJ, Madden DJ, Vaidya CJ, Howard DV, Howard JH Jr. Age-related differences in multiple measures of white matter integrity: a diffusion tensor imaging study of healthy aging. *Hum Brain Mapp*. 2010;31:378-390. doi:10.1002/hbm.20872
37. An L, Li S, Shen J. Simultaneous determination of metabolite concentrations, T1 and T2 relaxation times. *Magn Reson Med*. 2017;78:2072-2081. doi:10.1002/mrm.26612
38. Xin L, Schaller B, Mlynarik V, Lu H, Gruetter R. Proton T1 relaxation times of metabolites in human occipital white and gray matter at 7 T. *Magn Reson Med*. 2013;69:931-936. doi:10.1002/mrm.24352
39. Ethofer T, Mader I, Seeger U, et al. Comparison of longitudinal metabolite relaxation times in different regions of the human brain at 1.5 and 3 tesla. *Magn Reson Med*. 2003;50:1296-1301. doi:10.1002/mrm.10640
40. Wright AM, Murali-Manohar S, Borbath T, Avdievich NI, Henning A. Relaxation-corrected macromolecular model enables determination of 1H longitudinal T1-relaxation times and concentrations of human brain metabolites at 9.4T. *Magn Reson Med*. 2022;87:33-49. doi:10.1002/mrm.28958
41. Mlynárik V, Gruber S, Moser E. Proton T 1 and T 2 relaxation times of human brain metabolites at 3 tesla. *NMR Biomed*. 2001;14:325-331. doi:10.1002/nbm.713
42. Frahm J, Bruhn H, Gyngell ML, Merboldt KD, Hänicke W, Sauter R. Localized proton NMR spectroscopy in different regions of the human brain in vivo. Relaxation times and concentrations of cerebral metabolites. *Magn Reson Med*. 1989;11:47-63. doi:10.1002/mrm.1910110105
43. Hetherington HP, Mason GF, Pan JW, et al. Evaluation of cerebral gray and white matter metabolite differences by spectroscopic imaging at 4.1T. *Magn Reson Med*. 1994;32:565-571. doi:10.1002/mrm.1910320504
44. Deoni SCL, Peters TM, Rutt BK. High-resolution T1 and T2 mapping of the brain in a clinically acceptable time with DESPOT1 and DESPOT2. *Magn Reson Med*. 2005;53:237-241. doi:10.1002/mrm.20314
45. Schmitt P, Griswold MA, Jakob PM, et al. Inversion recovery TrueFISP: quantification of T1, T2, and spin density. *Magn Reson Med*. 2004;51:661-667. doi:10.1002/mrm.20058

46. Fujita S, Hagiwara A, Hori M, et al. Three-dimensional high-resolution simultaneous quantitative mapping of the whole brain with 3D-QALAS: An accuracy and repeatability study. *Magn Reson Imaging*. 2019;63:235-243. doi:10.1016/j.mri.2019.08.031
47. Koenig SH, Brown RD, Spiller M, Lundbom N. Relaxometry of brain: why white matter appears bright in MRI. *Magn Reson Med*. 1990;14:482-495. doi:10.1002/mrm.1910140306
48. Corrigan NM, Yarnykh VL, Hippe DS, et al. Myelin development in cerebral gray and white matter during adolescence and late childhood. *Neuroimage*. 2021;227:117678. doi:10.1016/j.neuroimage.2020.117678
49. Baadsvik EL, Weiger M, Froidevaux R, Schildknecht CM, Ineichen BV, Pruessmann KP. Myelin bilayer mapping in the human brain in vivo. *Magn Reson Med*. 2024;91:2332-2344. doi:10.1002/mrm.29998
50. Ma YJ, Jang H, Wei Z, et al. Myelin imaging in human brain using a short repetition time adiabatic inversion recovery prepared ultrashort Echo time (STAIR-UTE) MRI sequence in multiple sclerosis. *Radiology*. 2020;297:392-404. doi:10.1148/radiol.2020200425
51. van der Weijden CWJ, Biondetti E, Gutmann IW, et al. Quantitative myelin imaging with MRI and PET: an overview of techniques and their validation status. *Brain*. 2022;146:1243-1266. doi:10.1093/brain/awac436
52. Rae CD. A guide to the metabolic pathways and function of metabolites observed in human brain 1H magnetic resonance spectra. *Neurochem Res*. 2014;39:1-36. doi:10.1007/s11064-013-1199-5
53. Hoefemann M, Bolliger CS, Chong DGQ, van der Veen JW, Kreis R. Parameterization of metabolite and macromolecule contributions in interrelated MR spectra of human brain using multidimensional modeling. *NMR Biomed*. 2020;33:e4328. doi:10.1002/nbm.4328
54. Tal A. The future is 2D: spectral-temporal fitting of dynamic MRS data provides exponential gains in precision over conventional approaches. *Magn Reson Med*. 2023;89:499-507. doi:10.1002/mrm.29456
55. Zöllner HJ, Davies-Jenkins C, Simicic D, Tal A, Sulam J, Oeltzschner G. Simultaneous multi-transient linear-combination modeling of MRS data improves uncertainty estimation. *Magn Reson Med*. 2024;92:916-925. doi:10.1002/mrm.30110
56. Clarke WT, Ligneul C, Cottaar M, Ip IB, Jbabdi S. Universal dynamic fitting of magnetic resonance spectroscopy. *Magn Reson Med*. 2024;91:2229-2246. doi:10.1002/mrm.30001

How to cite this article: Murali-Manohar S, Zöllner HJ, Hupfeld KE, et al. Age dependency of neurometabolite T_1 relaxation times. *Magn Reson Med*. 2025;94:508-520. doi: 10.1002/mrm.30507